Biocatalytic Formation of Novel Polyesters with *para*-Hydroxyphenyl groups in the Backbone – Engineering *Cupriavidus necator* for production of high-performance materials from CO_2 and electricity

Nils JH Averesch[1,3]*, Vince E Pane[2,3], Frauke Kracke[1], Marika Ziesack[4,5], Shannon N Nangle[4,5], Pamela A Silver[4,6], Robert W Waymouth[2,3], Craig S Criddle[1,3]

(1) *Department of Civil and Environmental Engineering, Stanford University, CA, USA*
(1) *Department of Chemistry, Stanford University, CA, USA*
(3) *Center for the Utilization of Biological Engineering in Space, CA, USA*
(4) *Wyss Institute for Biologically Inspired Engineering, MA, USA*
(5) *Circe BioScience, MA, USA*
(6) *Harvard Medical School, MA, USA*

* Correspondence: nils.averesch@uq.net.au

Abstract

Synthetic materials are integral components of consumables and durable goods and indispensable in our modern world. Polyesters are the most versatile bulk- and specialty-polymers, but their production is not sustainable, and their fate at end-of-life of great concern. Bioplastics are highly regarded alternatives but have shortcomings in material properties and commercial competitiveness with conventional synthetic plastics. These constraints have limited the success in global markets. Enabling bio-production of advanced bioplastics with superior properties from waste-derived feedstocks could change this.

We have created microbial cell factories that can produce a range of aliphatic and aromatic polyesters. A Δ*phaC1* mutant of *Cupriavidus necator* H16 was complemented with hydroxyacyl-CoA transferases from either *Clostridium propionicum* (*pct540*) or *Clostridium difficile* (*hadA*), respectively. These were combined with a mutant PHA synthase (*phaC1437*) from *Pseudomonas* sp. MBEL 6-19, which rescued the PHA^- phenotype of the knock-out mutant and allowed polymerization of various hydroxy carboxylates, including phloretic acid. This is the first-time, incorporation of an aromatic ring in the backbone of a biological polyester was achieved. Polymers contain *para*-hydroxyphenyl subunits are structurally analogous to synthetic aromatic polyesters like PET and high-strength polyarylates.

In a further advance, the transgenic strain was cultivated in a bio-electrochemical system under autotrophic conditions, enabling synthesis of aromatic bio-polyesters from H_2 and O_2 generated *in situ*, while assimilating CO_2. Follow-up elementary flux-mode analysis established the feasibility of *de novo* production of twenty different polyesters from five different carbon- and energy-sources. This comprehensive study opens the door to sustainable bio-production of high-performance thermoplastics and thermosets.

Significance statement

New biomaterials can facilitate transition to a carbon-neutral chemical industry and a circular economy while at the same time preventing accumulation of plastic wastes in the environment. This can be accomplished by developing "drop-in" replacements for existing fossil carbon-based plastics. To that end, this work demonstrates for the first time that biocatalytic polymerization can incorporate an aromatic *para*-hydroxyphenyl carbonic acid into the backbone of a bio-polyester. This was accomplished using a genetically engineered microbial cell factory that assimilates carbon dioxide using hydrogen that is produced electrochemically *in situ*. A bio-electrochemical system eliminates the need for external supply of oxyhydrogen and avoids explosive mixtures, opening the door for sustainable production of biomaterials analogous to aromatic bulk-polyesters such as PET and high-performance "liquid-crystal polymers".

Highlights

- Biocatalytic formation of aromatic polyesters with structural analogy to polyarylates
- Production of novel PHAs from CO_2 and H_2+O_2 produced *in situ* in a bio-electrochemical system
- Expression-level of PHA synthase and molecular weight of polyesters are inversely correlated
- *In silico* design and analysis of pathways towards novel PHAs from different carbon-sources

Keywords

Polyhydroxyalkanoates, aromatic polyesters, bioplastics, C-1 feedstocks, microbial electrosynthesis

Abbreviations

3HP, 3-hydroxypropionic acid; 4HB, 4-hydroxybutyric acid; 6HC, 6-hydroxycaproic acid; BES, bio-electrochemical system; BM, biomass; CDW, cell dry weight; DAP diaminopimelate; DSC, differential scanning calorimetry; EMA, elementary flux-mode analysis; GC-MS, gas chromatography–mass spectrometry; GPC, gel permeation chromatography; HA, hydroxy acid; MA, mandelic acid; MES, microbial electrosynthesis; M_n, number-average molecular weight; MSM, mineral salts medium; M_W, weight-average molecular weight; NMR, nuclear magnetic resonance; OD, optical density; PA, phloretic acid; PDI, polydispersity index; PET, polyethylene terephthalate; PHA, polyhydroxyalkanoate; PHB, polyhydroxybutyrate; PHBV, polyhydroxybutyrate-co-hydroxyvalerate; PheLA, phenyllactic acid; PLA, polylactic acid; RB, rich broth; rpm, rounds per minute; VFA, volatile fatty acid;

Introduction

Background

Modern society is based upon ever-increasing consumption of energy and material resources. The outcome is ever-increasing emissions of waste and pollutants (1, 2). Greenhouse gases have reached critical levels, and pollution fabrication of recalcitrant synthetic materials is ubiquitous and undeniable. A lifestyle and an economy dependent upon plastic consumption risks serious harm to the biosphere (3). To ensure a viable planet for generations to come, methods are needed to reduce waste accumulation while embracing readily available and renewable feedstocks (4). While plastic recycling is necessary for a circular economy, recycling alone will not prevent unintended release of synthetic materials into the environment. This is especially the case in single-use applications where the stability of plastics is as unnecessary as it is problematic (5). Bio-degradable materials derived from renewable feedstocks or from upcycling of existing materials are desirable (6) but materials derived from cultivated feedstocks are not necessarily climate friendly (7). Utilization of low-cost (waste) carbon-sources, such as C1-feedstocks for production of materials can potentially directly mitigate greenhouse gas emissions while avoiding competition with the food-industry (8). Such a strategy improves commercial competitiveness by decreasing feedstock cost (9). Especially useful are compounds that can substitute for or directly replace industrial (petrochemistry-based) polymers. Such bio-replacements are attractive because they do not require extensive modifications to the existing infrastructure for processing and manufacturing (minimal CapEx).

Polyhydroxybutyrate (PHB), a biological thermoplastic polyester, can be produced outgoing from non-edible, waste-derived carbon-sources, such as carbon dioxide or methane and could be a bio-degradable replacement for synthetic materials (10). Shortcomings in its material properties (11) and high production cost (9) have, however, hampered its adoption. This has been addressed, in part, by addition of co-monomers that can tune material properties and generate a multitude of polyhydroxyalkanoates (PHAs) (11). The most prominent one, PHBV, is based on valeric acid, which is easily incorporated and benefits material properties, however, as an odd-number carbonic acid not readily bio-available. Alternatives exist, in particular, linear, short-chain PHAs have properties like high strength and flexibility that make them attractive and viable for specialty applications (12-14). PHAs with aromatic groups (in the side chain) have a wide range of properties, which are, however, hard to predict as they do not scale linearly with the fraction of aromatic co-monomer (15). In general, they are more amorphic than the highly crystalline PHB and therefore have increased glass-transition and higher degradation temperatures, allowing for a wider processing window. Specifically, poly(mandelite) (16) and poly(phenyllactide) (17), polymers of mandelic and phenyllactic acid, respectively, have been chemically synthesized and characterized, and these materials exhibit properties mimicking those of polystyrene. Recently, biological production of aromatic hydroxy acids from sugar and their incorporation into PHB co-polymers has been demonstrated through metabolic engineering of *Escherichia coli* (18).

To date, all biocatalytically produced aromatic PHAs have contained the aromatic ring on a side chain (15). Incorporation of the aromatic ring into the backbone of the bio-polyester would conceivably result in vastly altered properties, yielding structural analogs to e.g., polyethylene terephthalate (PET) and polyarylates. Analog polyesters have been chemically synthesized and characterized based on natural hydroxy acids, e.g. glycolic and *para*-hydroxybenzoic acid (19), as well as 3-(*para*-hydroxyphenyl)propionic (phloretic) and 3-(*para*-hydroxyphenyl)acrylic acid (coumaric) acid (20). These "polyhydroxyarylates" exhibited liquid-crystal polymer properties and are potentially biodegradable.

Concept

This work explored microbial production of a wide range of thermoplastic materials from sustainable feedstocks *in -vivo* and *in -silico*. The chemolithoautotrophic 'knallgas' bacterium *Cupriavidus necator* was selected as chassis organism, as it is an excellent producer of bio-polyesters and can utilize various carbon- and energy-sources, including carbon dioxide and oxyhydrogen (21). This well-characterized mixotroph grows rapidly to high cell densities and has previously been engineered for production of non-natural PHAs, including fatty acid-derived medium chain-length poly(3-hydroxyalkanoate)s and lactic acid co-polymers, outgoing from CO_2 and sustainable carbon-sources (22, 23), as well as aromatic PHAs from externally supplied precursors (24). Expanding upon these previous studies, a Δ*phaC1* knock-out mutant of *C. necator* H16 was complemented with the genes for a hydroxyacyl-CoA transferase (*pct540* or *hadA* from *Clostridium propionicum* or *Clostridium difficile*, respectively) and evolved PHA synthase (*phaC1437* from *Pseudomonas* sp. MBEL 6-19)), which had previously been employed for production of aromatic PHAs in a different context (18, 25). This allowed biosynthesis and subsequent characterization of several straight chain aliphatic and aromatic PHAs by complementing and repurposing natural *poly*(3-hydroxbutyrate) (PHB) synthesis (cf. figure 1).

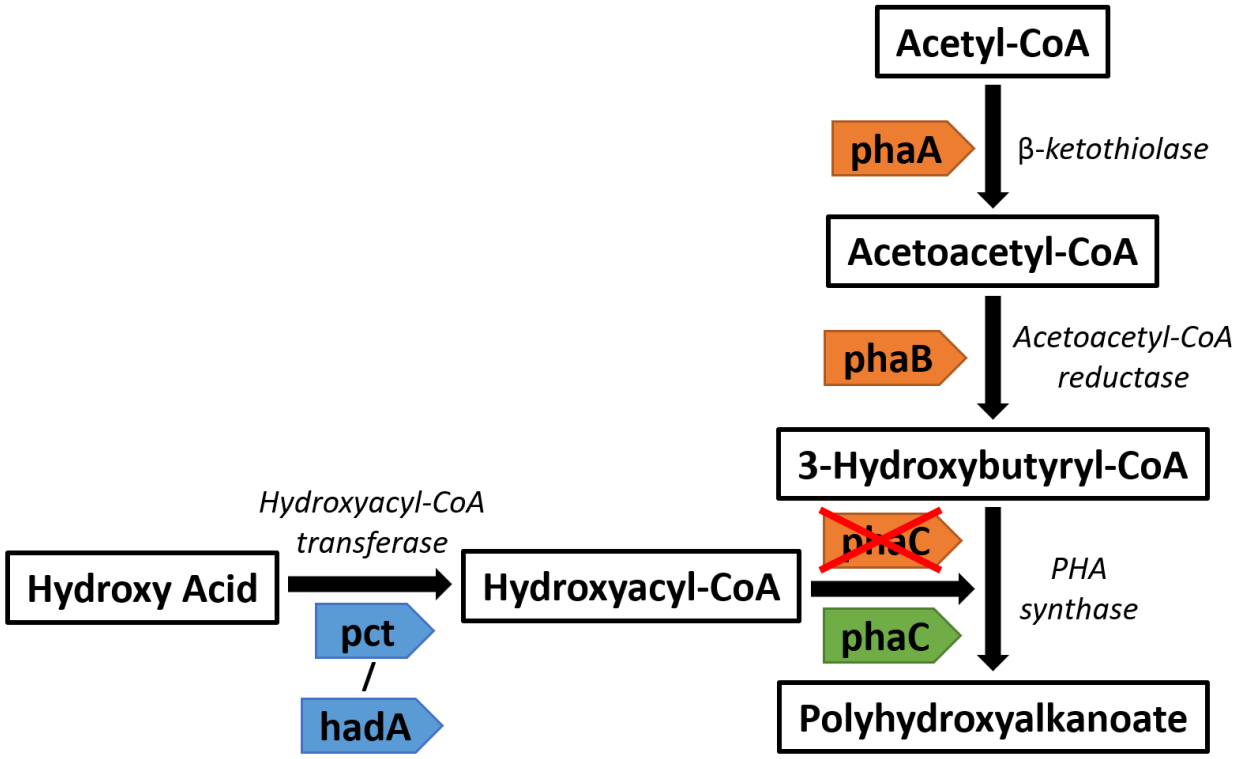

Figure 1: Partial breakdown of natural biochemical pathway for *poly*(3-hydroxybutyrate) synthesis (vertical) and synthetic biochemical pathway for formation of modified bio-polyesters (horizontal). Involved genes (in chevrons) are highlighted orange for natural, or blue (CoA transferase, *pct* / *hadA*) and green (PHA synthase, *phaC*), respectively, in case of heterologous (manually introduced) genes.

Results and Discussion

Formation of Non-Natural Polyesters from Externally Supplemented Precursors

Introduction of the heterologous PHA synthase into *C. necator* H16 Δ*phaC1* could rescue the PHB-negative phenotype of the knock-out mutant. Per-biomass yield was comparable to the wild-type (≈ 60% $w_{PHA}/w_{BIOMASS}$, data not shown); remarkably, bio-polyesters were formed independent of induction (P_{BAD}) of expression of the heterologous genes, merely by limiting the Nitrogen-source. Nuclear magnetic resonance (^{1}H-NMR) spectroscopy revealed that the polymer was composed of 3-hydroxybutyrate with small fractions of other hydroxy acids, likely derivatives of higher fatty acids.

Several rounds of feeding experiments with various hydroxy carbonates were conducted in batch (shake-flask) cultures. The composition of the obtained polyester, as well as the respective fraction of non-natural monomers in the co-polymer were determined by means of gas-chromatography coupled mass-spectroscopy (GC-MS), as well as ^{1}H-NMR spectroscopy, which was in certain cases complemented with ^{13}C-NMR spectroscopy. The different polyesters that were formed from the hydroxy acids supplemented in the growth medium, and the ratios of the different repeat units are given in table 1.

Table 1: Polymers obtained from feeding experiments of *C. necator* H16 (wild-type and engineered strains) with precursors and fraction of non-natural monomer in the obtained co-polyester. Ratios are based on ^{1}H-NMR spectroscopy, those obtained from GC-MS can be found in supplementary material 1.

Precursor / Concentration		Strain / co-polymer & ratio of repeat units		
		H16 (wild-type)	H16 Δ*phaC1* Δ*phaC1 pct540 phaC1437*	H16 Δ*phaC1 hadA phaC1437*
–	N/A	*P*3HB	*P*3HB	*P*3HB
glycolic acid	20 mM	*P*3HB	*P*3HB	*P*3HB
D-lactic acid	20 mM	*P*3HB	*P*3HB	*P*3HB
3-hydroxypropionic acid	20 mM	*P*3HB	*P*(3HB-*co*-3HP) ≈100:12[$]	*P*(3HB-co-3HP) ≈100:1[$]
4-hydroxybutyric acid	20 mM	*P*(3HB-*co*-4HB) ≈100:9	*P*(3HB-*co*-4HB) ≈1:1	*P*(3HB-*co*-4HB) ≈10:1
6-hydroxycaproic acid	<10 mM*	*P*(3HB-*co*-4HB) ≈100:13	*P*(3HB-*co*-4HB) ≈100:13:8	*P*(3HB-*co*-4HB-*co*-6HC) ≈100:5:2
2-hydroxy-4-phenylbutyric acid	10 mM	n.d.	*P*3HB	*P*(3HB-*co*-2H4PheB) ≈20:1
D-phenyllactic acid	10 mM	n.d.	*P*3HB	*P*(3HB-*co*-PheLA) ≈2:1
mandelic acid	5 mM	n.d.	*P*3HB	*P*(3HB-*co*-MA) ≈4:1
phloretic acid	5 mM	n.d.	*P*3HB	*P*(3HB-*co*-PA) ≈100:1

* approx. 10 mM supplied, above solubility limit, [$] only NMR, unconfirmed by GC-MS. Abbreviations: n.d. = not determined, 3HP = 3-hyroxypropionate, 3HB = 3-hydroxybutyrate, 4HB = 4-hydroxybutyrate, 6HC = 6-hydroxycaproate, 2H4PheB = 2-hydroxy-4-phenylbutyrate, PheLA = phenyllactate, MA = mandelate, PA = phloretate.

Throughout the batch cultivations, which were conducted on fructose as carbon- and energy-source (for experimental simplicity), some of the polymer-precursors exhibited toxicity, which dictated the maximum deployable concentrations, as per table 1. In particular, the hydroxypropionic acids affected the growth rate negatively (data not shown). While not toxic, poor solubility of 6-hydroxycaproic acid (< 10 mM) limited the final concentration of the ω-fatty acid in the growth medium. The aromatic hydroxy acids also appeared to be rather toxic, esp. 2-hydroxy-4-phenylbutyric (2H4PheB) and mandelic acid (MA) could only be supplied at 10 mM and 5 mM, respectively, if not to inhibit growth completely.

No co-polymers containing glycolic and lactic acid were obtained. It is likely that these short organic acids were catabolized before they could be polymerized, as these volatile fatty acids (VFAs) are known to be good substrates for *C. necator* (26-28). The presence of co-polymers with 3-hydroxypropionic acid (3HP) is ambiguous: while ^{1}H-NMR spectra were in good accordance with literature (29) (triplet resonance at 4.33 ppm indicative of the C3-methylene), GC-MS could not confirm the presence of *P*(3HB-*co*-3HP). Incorporation-level of 4-hydroxybutyric acid (4HB) by the engineered strain that carried *hadA* and *phaC1437* and by the wild-type was similar (≈ 10%), indicating that (a) *C. necator*'s native CoA transferase "YdiF" / *pct* accepts 4HB well enough (30) and (b) the natural PHA synthase (*phaC1*) is promiscuous enough to polymerize the non-natural hydroxy carbonic acid. Deducted therefrom it appears that the heterologous enzymes offer no significant advantage for formation of a 4-hydroxybutyrate co-polymer over the native ones. GC-MS, however, did not detect any non-natural PHAs in control experiments with the wild-type (cf. supplementary material 1, Table S2).

Importantly, the strain carrying *pct540* and *phaC1437* produced a co-polymer with a high fraction of 4HB (approx. 66%, cf. figure 3A). NMR and GPC further indicated that the obtained polyester was a block-co-polymer. The strain showed considerably reduced growth, as compared to the wild-type or the other transgenic mutant, but only when expression was induced. The retardation of growth correlated with the onset of expression; fructose consumption also came to a halt at that point (cf. supplementary material 1, figures S1, S2 & S3, S4). This indicates severe protein toxicity, which is a known problem of propionyl-CoA transferases (25). Altogether, it seems that overall metabolism stalled, which would also have halted 3-hydroxybutyrate (3HB) formation. The high 4HB content in the PHA produced by the *pct540* strain is potentially a result of that effect, rather than the heterologous function(s) of the expressed enzyme(s). This hypothesis can also explain the block-co-polymer – while in the beginning (pre-induction) a polymer that is mostly constituted of intracellular 3HB would be (constitutively) produced, in the end (after induction) 3HB would deplete, allowing only pure catalysis to take place, solely adding externally provided 4HB to the polymer chain. This also explains the comparatively high PDI (~3, cf. supplementary material 1, Table S1) of the co-polymer, which is a result of the polymers heterogeneity (size differences between the different chains).

When supplying 6-hydroxycaproic acid (6HC), the engineered strains and the wild-type both formed non-natural PHAs: while the wild-type produced a co-polymer containing 4HB, the PHA derived from the engineered strain contained 4HB and 6HC (cf. figure 3B). In all cases presence of 4HB is attributed to the original C6 ω-fatty acid undergoing β-oxidation to a C4 ω-fatty acid. In the engineered strain the highly active heterologous PHA synthase, potentially in concert with the over-expressed CoA transferase, accelerates formation of the polymer, partially outcompeting β-oxidation. This was only observable from NMR spectroscopy, GC-MS analysis did not show any incorporation of 6HC into the PHA by the wild-type, nor 4HB in samples from cultures where 6HC was supplied as precursor.

Aromatic hydroxy acids were incorporated into the polymer only by the strain carrying *hadA* and *phaC1437*. Significant aromatics content was obtained, and fractions differed depending on the precursor: while external supply of 2H4PheB yielded a polymer with a fraction of the aromatic one order of magnitude lower than 3HB (cf. figure 3C), incorporation of phenyllactic acid (PheLA) yielded a PHA that contained a high fraction (same order of magnitude as 3HB) of aromatic repeat unit (cf. figure 3D). This led to drastically changed polymer properties, including reduced melting point and increased solubility (e.g., readily soluble in acetone). The dry polymer appeared ductile at room temperature. The polymer obtained from MA (cf. figure 3E) had about half the aromatics content of the PheLA co-polymer, which may be attributed to the lower (half) concentration of precursor that was supplied.

Most significantly, also the *para*-hydroxyphenyl compound 'phloretic acid' was successfully polymerized by the *hadA*-strain (cf. figure 3F). Albeit only a minor fraction of the aromatic compound was incorporated into the backbone of the bio-polyester, to our knowledge it is the first-time something like this has been accomplished, paving the way to a new class of bio-available materials: co-polymers with the aromatic ring in the backbone have structural analogy to polyarylates. In future, homopolymers or co-polymerization of *para*-hydroxyphenyl or *para*-hydroxybenzoic acids with straight-chain aliphatic hydroxy acids could generate high-performance materials with structural analogy to e.g., PET or liquid crystal polymers like Vectran™.

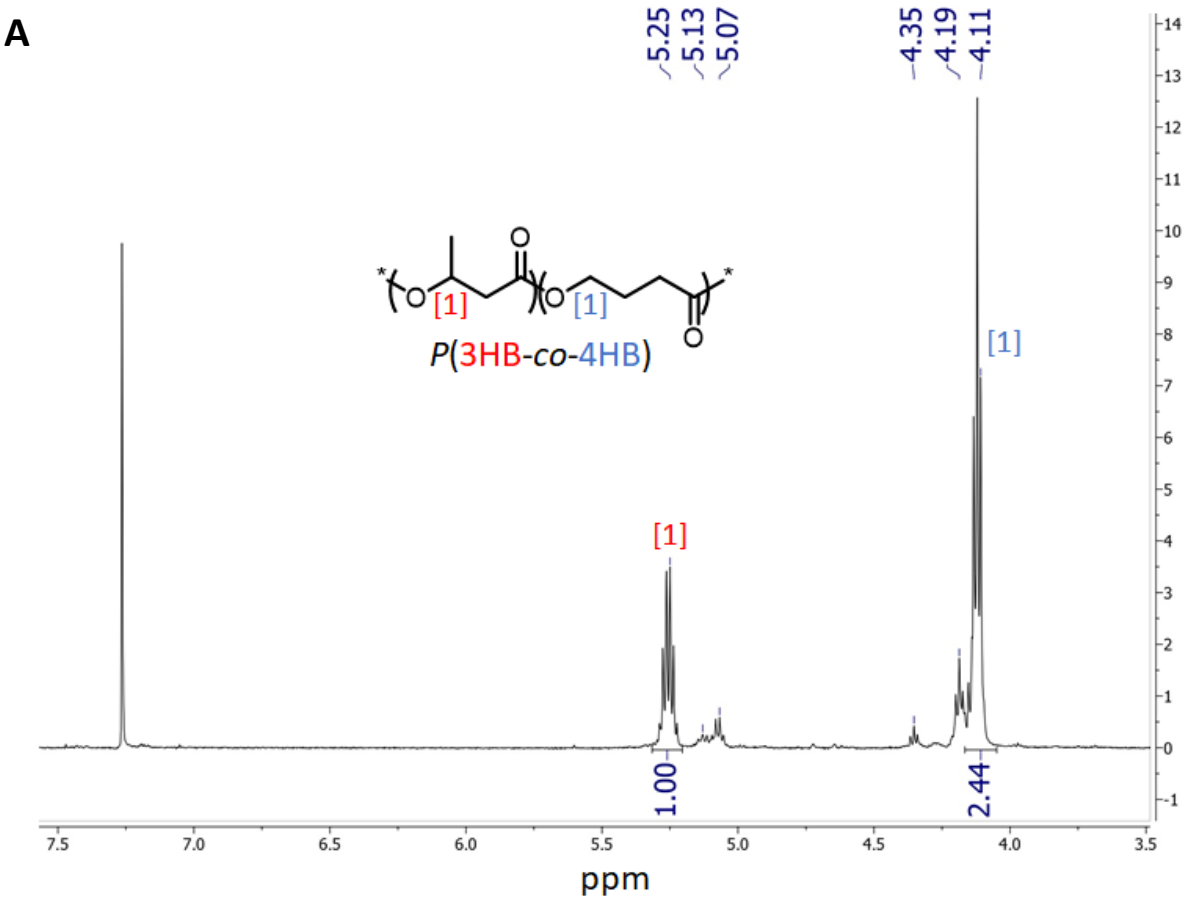

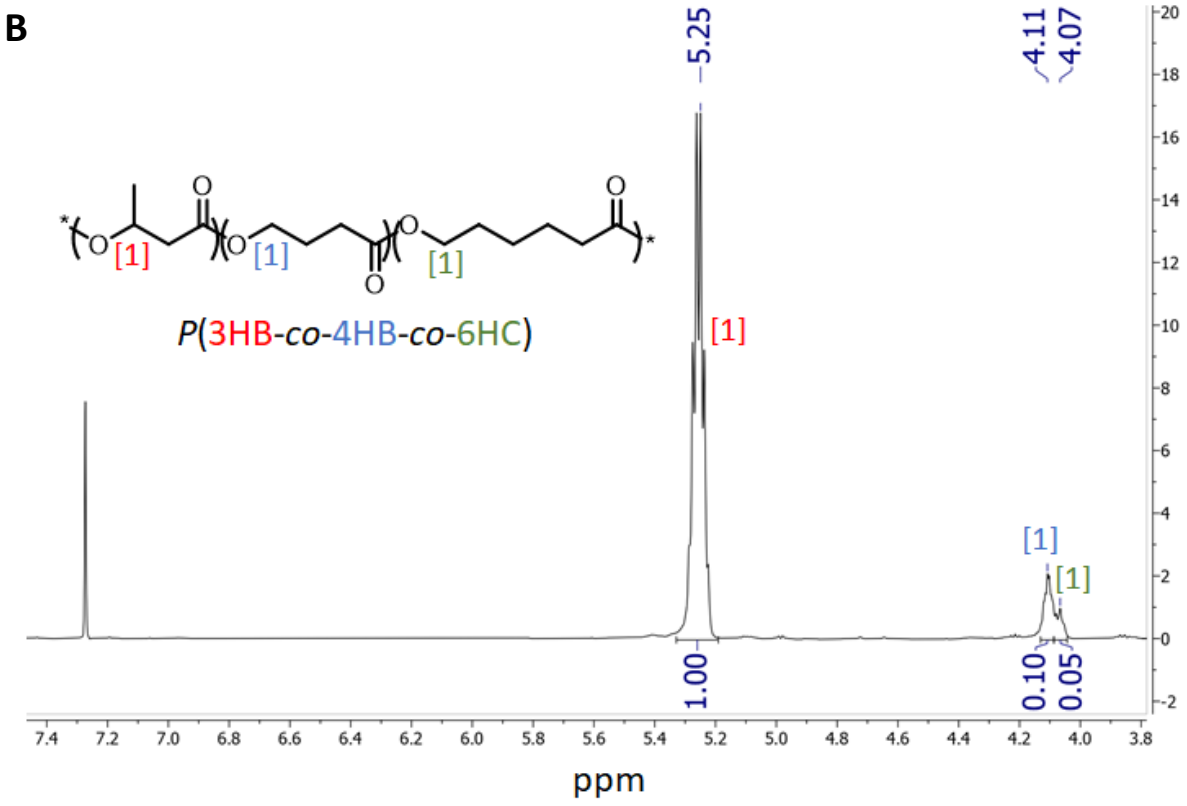

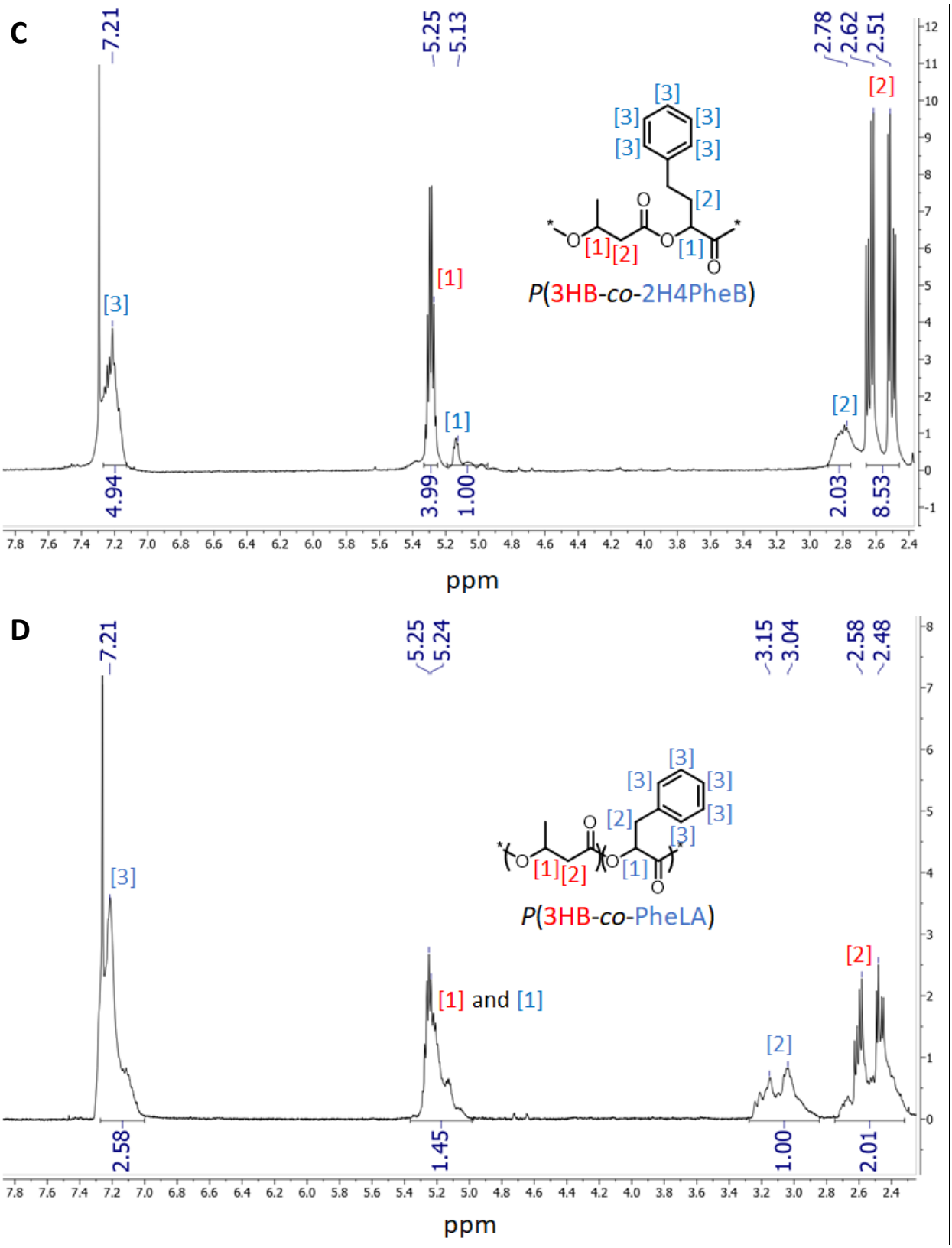

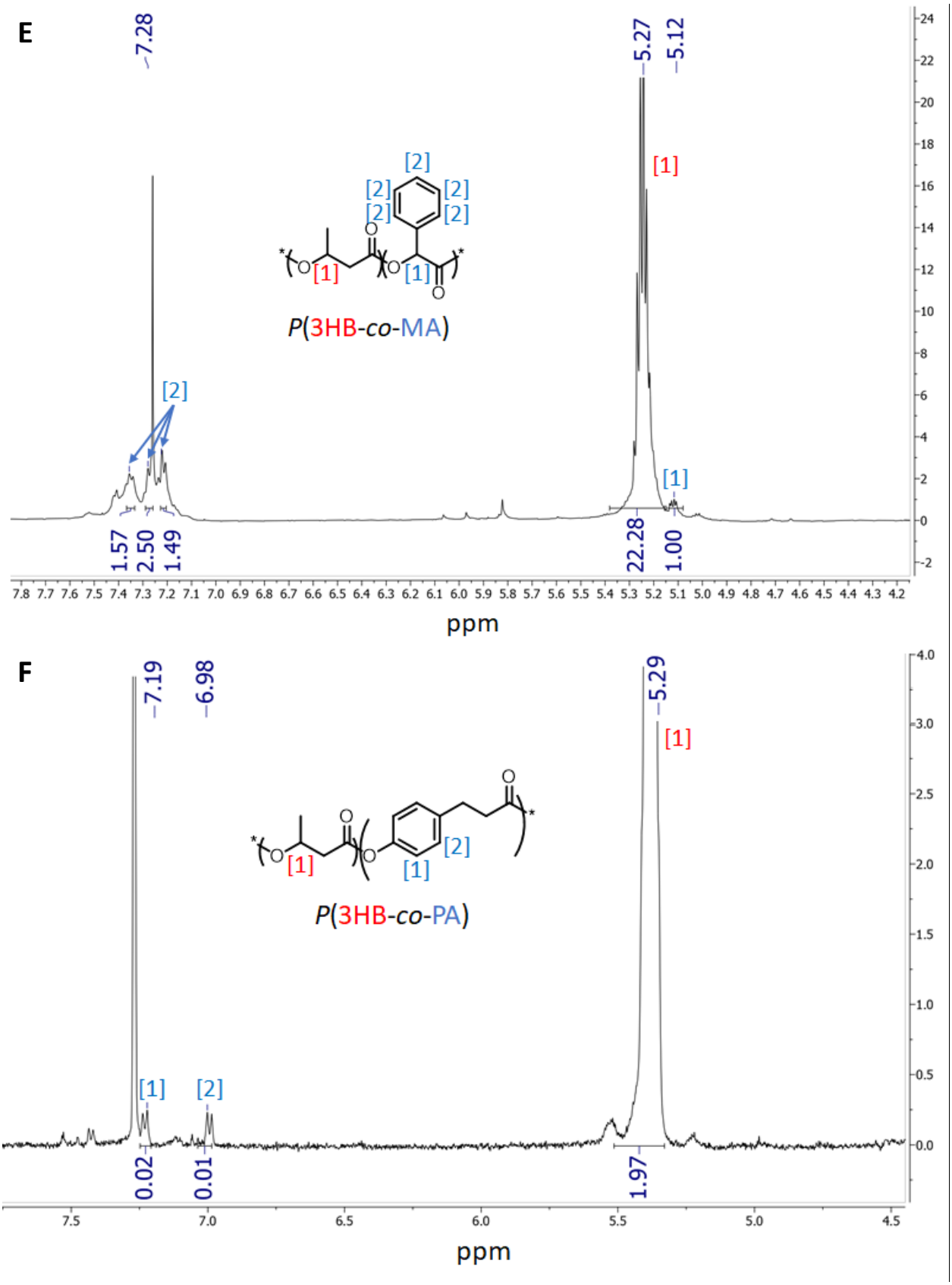

Figure 3: ^{1}H-NMR spectra of *P*(3HB-*co*-4HB) produced by *C. necator* H16 Δ*phaC1* pCM66T_P$_{BAD}$-*pct540-phaC1437* (A) as well as *P*(3HB-*co*-4HB-*co*-6HC) (B), *P*(3HB-*co*-2H4PheB) (C), *P*(3HB-*co*-PheLA) (D), *P*(3HB-*co*-MA) (E), and *P*(3HB-*co*-PA) (F) produced by *C. necator* H16 Δ*phaC1* pCM66T_P$_{BAD}$-*hadA-phaC1437*. Areas are indicative of the ratios for 3HB to non-natural repeat units. (A): In addition to the P3HB sextet resonance at 5.25 ppm, a triplet resonance at 4.11 ppm shows that the C4-methylene of the 4HB repeat is present, indicating incorporation of 4HB into the polymer. The large fraction of P4HB causes multiple P3HB peaks because of different possible orders in the polymer (e.g., -3HB-P3HB-P4HB-, -P4HB-P3HB-P4HB-, -P4HB-P3HB-P3HB-, -P3HB-P4HB-P3HB-). (B): In addition to the P3HB sextet resonance at 5.25 ppm and P4HB triplet resonance at 4.11 ppm, a triplet resonance at 4.07 ppm shows that the C6-methylene of the 6HC repeat is present, indicating incorporation of 6HC into the polymer. (C): In addition to the P3HB sextet resonance at 5.25 ppm, a triplet resonance at 5.13 ppm shows that the C2-methine of the 2H4PheB repeat is present. The broad aromatic multiplet resonance at 7.21 ppm is also indicative of P2H4PheB. (D): The P3HB sextet resonance at 5.25 ppm overlaps with the methine PPheLA resonance, so the methylene doublet resonances of 3.15 & 3.04 ppm and 2.58 & 2.48 ppm were used to show the presence of P3HB and PPheLA respectively. The broad aromatic resonance at 7.21 ppm is also indicative of PPheLA. (E): In addition to the P3HB sextet resonance at 5.25 ppm, a multiplet resonance at 5.12 ppm shows that the C2-methine of the MA repeat is present. The broad aromatic multiplet resonance at 7.28 ppm is also indicative of MA. (F): In addition to the P3HB sextet resonance at 5.25 ppm, two doublet resonances at 7.19 and 6.98 ppm show that the aromatic PA repeat is present, indicating incorporation of the *para*-hydroxyphenyl unit into the polymer.

Impact of Genetic Engineering on PHB Production and Composition

We further characterized PHB production of the genetically engineered strains in comparison to the wild-type *C. necator* H16. The molecular weight of polymer produced by the transgenic strain was compared to the polymer derived from wild-type *C. necator* H16 by means of gel-permeation chromatography (GPC): bio-polyester derived from the engineered strain (not induced) was approx. 5-times lower M_W (or M_n) than that produced by the wild-type (figure 2). Induction of the engineered strain (i.e., over-expression of the heterologous genes) resulted in another 5-fold reduction in molecular weight of the produced polymer. It thus appears that enzyme expression-level and polymer chain-length are inversely correlated.

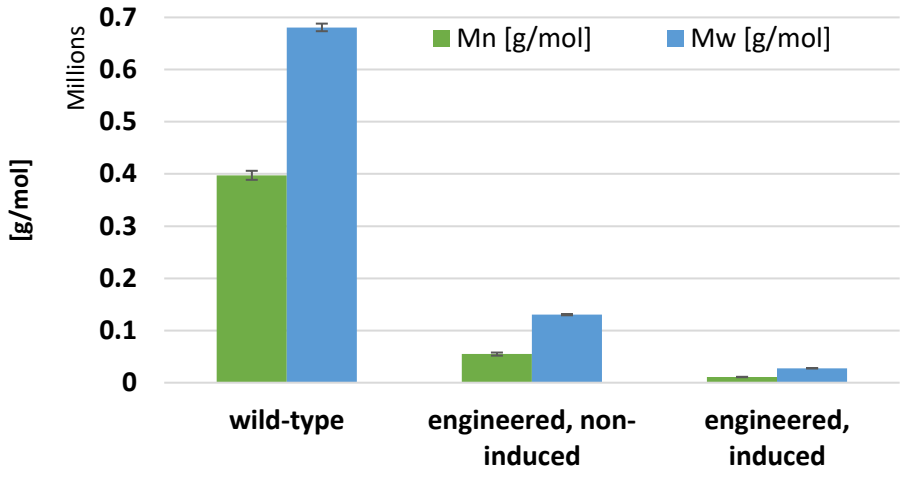

Figure 2: Molecular weight distribution (M_n and M_W) for PHA obtained from wild-type *C. necator* H16, and engineered *C. necator* H16 (Δ*phaC1* pCM66T_P$_{BAD}$-*hadA-phaC1437*, non-induced and fully induced, respectively).

To determine the cause of this correlation, expression-levels of the PHA synthase (and CoA transferase) during induced and non-induced conditions were compared qualitatively. In the latter case the proteins were not detected (cf. supplementary material 1, figures S1 & S2), albeit catalytic activity of the PHA synthase apparently existed. The hypothesis is that the PHA synthase is highly active so that even very low (leaky) expression (that is virtually non-detectable) allows for formation of PHA. This would also explain the reduction in molecular weight of the polymer when expression is fully induced, as the high activity in combination with high abundance of the catalyst could lead to (local) depletion of substrate and subsequently premature termination of chain-elongation. A congruent phenomenon has been described when shuffling gene order of the natural *phaCAB* operon (31).

The molecular weight of other non-natural (aromatic) PHAs was in the same order of magnitude as for the PHB from the transgenic strains, as was the inverse correlation between enzyme expression and polymer molecular weight. The PDI of non-natural polyesters was generally higher than that of natural PHB (natural < 2 < non-natural), where PDIs where highest in cases where enzyme expression was induced. Hence, it appears that tight, individual, and carefully balanced control of the expression-levels of the enzymes is compulsory in order to fine-tune polymer quality. Extended data containing the M_W, M_n and PDI of the different PHAs can be found in the supplementary material 1.

Autotrophic production of Aromatic Polyesters in Bio-electrochemical System

C. necator derives the electrons required for reduction and subsequent assimilation of carbon dioxide from molecular hydrogen. Aerobic gas-fermentation, however, is costly and involves serious safety concerns. Therefore, innovative solutions have been proposed that allow *in-situ* formation of H_2 via electrochemical water splitting in a bio-electrochemical system (BES) (32-34). To demonstrate the sustainable production of novel aromatic polyesters via microbial electrosynthesis (MES), engineered *C. necator* H16 Δ*phaC1* pCM66T_P_{BAD}-*hadA-phaC1437* (hadA-strain) was cultivated in a single-chamber BES with CO_2 and electrical current (to generate oxyhydrogen *in-situ*) as only inputs (Figure 4, see also supplementary material 1, Figure S5). In the membrane-less system, a constant current was applied, which led to water being split into oxygen at the anode and hydrogen at the cathode. CO_2 was continuously purged into the reactor, providing a gas-mix for chemolithotrophic growth of *C. necator*. The BES was inoculated from a culture grown on a gaseous $H_2/CO_2/O_2$ mixture to facilitate adaptation to electroautotrophic conditions, which resulted in immediate growth in the BES (cf. Figure 4) with no lag-phase. Preliminary experiments (data not shown) suggested that the amount of nitrogen-source to achieve limiting-conditions and initiate PHA accumulation was critical in the BES. Consequently, the concentration of ammonium salt in the medium was reduced and monitored throughout the experiment. Polymer precursor (PheLA) was added in two steps to minimize toxic effects. Under conditions of MES, growth rate was lower as compared to growth on gas (BES: $t_D \approx 26$ h vs. serum-bottles: $t_D \approx 10$ h, data not shown), which can be explained with mass-transfer limitations in the BES (ambient pressure and limited agitation). Nevertheless, significant biomass was accumulated, exceeding batch-experiments in serum-bottles: a maximum OD_{600} of 6.2, corresponding to a biomass concentration of ≈ 1.8 g/L, was reached after 90 h. The culture was harvested after 140 h and extraction of polyesters yielded an aromatic polyester, which was identified as *P*(3HB-*co*-PheLA) by means of ^{1}H-NMR spectroscopy. The content of non-natural monomer was lower than on fructose (48:2 under autotrophic vs. 2:1 under heterotrophic conditions, for 3HB to PheLA), which could be explained with lower concentration of precursor (1/4th i.e., 5 mM PheLA) and inducer (1/10th i.e., 0.1 g/L arabinose) in the microbial medium, as well as limited energy available to metabolism under autotrophic conditions (21). Nevertheless, this demonstrates feasibility to produce these novel polymers from C1-feedstocks and electrical energy, which could electrify the materials industry and, when powered by renewable sources, would further close the loop to integrate this sector into a circular economy (2).

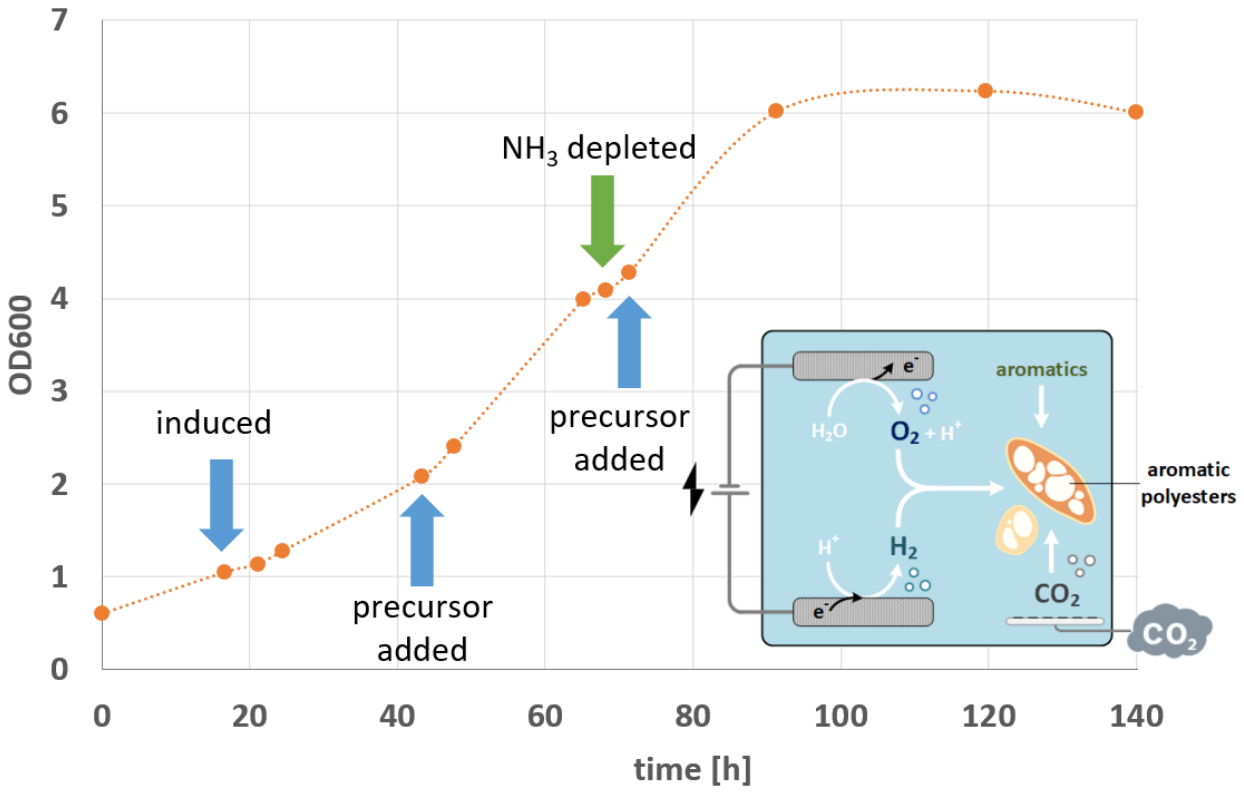

Figure 4: Cultivation-profile (growth by means of OD) of representative experiment with transgenic *C. necator* H16 Δ*phaC1* pCM66T_P_{BAD}-*hadA-phaC1437* in bio-electrochemical system (BES). Induction of expression, addition of aromatic polymer-precursor and depletion of nitrogen source as indicated. The insert on the bottom right shows a schematic of the BES, which evolves H_2 at the cathode and O_2 at the anode as electron carrier and acceptor for autotrophic growth and production of aromatic polyesters from CO_2 and electricity.

Assessing Biosynthesis of Novel Bio-Polyesters through Metabolic Modelling

In support of the efforts described above, an *in silico* analysis was conducted to assess feasibility of *de novo* production of the obtained co-polymers solely from basic carbon-sources. For simplification, only homo-polymers where considered. A reconstructed metabolic model of *C. necator* was amended with biochemical pathways for formation of several aliphatic or aromatic hydroxy acids and polymerization thereof, which in some cases were hypothetical (cf. supplementary material 1, figure S6 and supplementary material 3). Using elementary flux-mode analysis (EMA), the production capacity for the different (non-natural) polyesters was compared on fructose, glycerol, acetate, formate and carbon dioxide + hydrogen, in terms of maximum theoretical product yield. The results are shown in Figure 5, the corresponding numerical carbon-yields can be found in supplementary material 3.

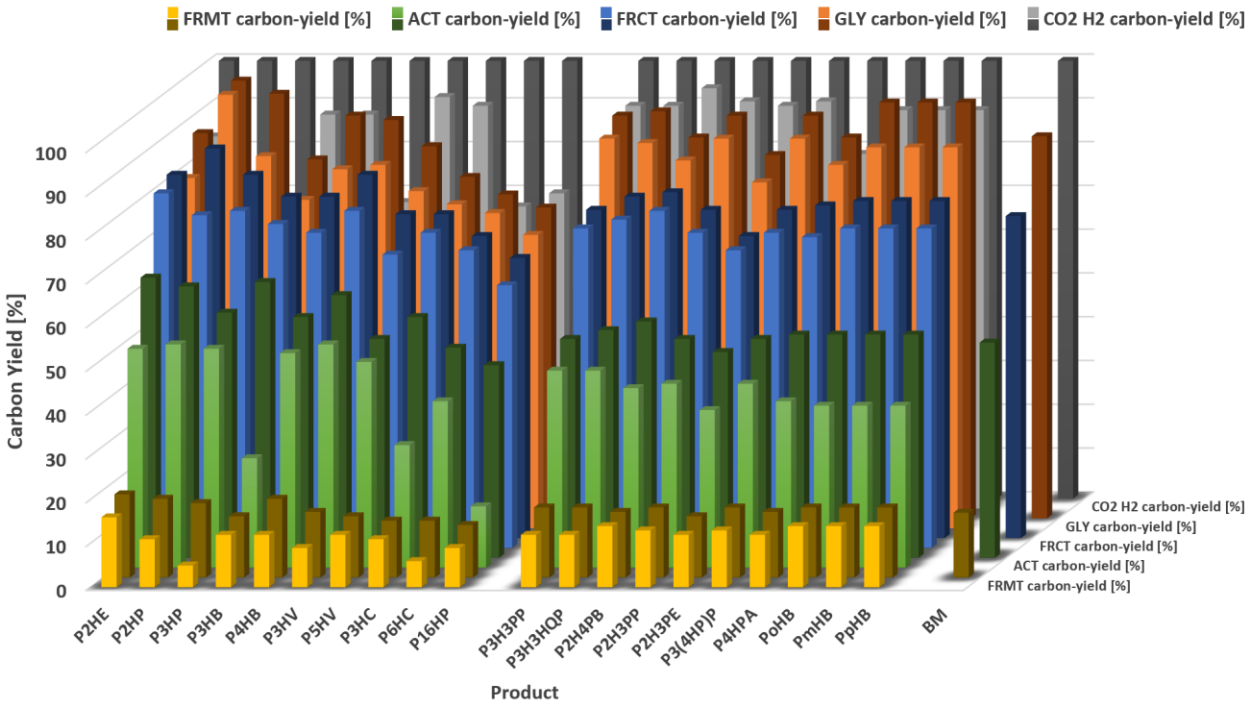

Figure 5: Theoretical maximum carbon-yields for a range of aliphatic as well as aromatic PHAs, producible from different carbon-/ energy-sources with engineered *C. necator*. Lighter shaded bars are product carbon-yields that allow for simultaneous growth, while darker shaded bars are absolute maximum theoretical product carbon-yields. The far-right columns represent the absolute maximum biomass yields, obtainable on the different carbon-sources. Substrates: FRMT = formate, ACT = acetate, FRC = fructose, GLY = glycerol; CO2 H2, carbon dioxide + hydrogen. Products: P2HE = poly(2-hydroxyethanoate), P2HP = poly(2-hydroxypropanoate) [poly(lactate)], P3HP = poly(3-hydroxypropanoate), P3HB = poly(3-hydroxybutyrate), P4HB = poly(4-hydroxybutyrate), P3HV = poly(3-hydroxyvalerate), P5HV = poly(5-hydroxyvalerate), P3HC = poly(3-hydroxycaproate), P6HC = poly(6-hydroxycaproate), P16HP = poly(16-hydroxypalmitate), P3H2PP = poly(3-hydroxy-3-phenylpropanoate), P3H2HQP = poly(3-hydroxy-3-hydroquinoyl-propanoate), P2H4PB = poly(2-hydroxy-4-phenylbutanoate), P2H3PP = poly(2-hydroxy-3-phenylpropanoate) [poly(phenyllactate)], P2H3PE = poly(2-hydroxy-3-phenylethanoate) [poly(mandelate)], P3(4HP)P = poly(3-(4-hydroxyphenyl)propanoate) [poly(phloretate)], P4HPA = 4-hydroxyphenylacetate, PoHB = poly(*orth*-hydroxybenzoate), PmHB = poly(*meta*-hydroxybenzoate), PpHB = poly(*para*-hydroxybenzoate), BM = biomass.

Bio-production of all considered aliphatic as well as aromatic PHAs for whom biochemical reactions exist that allow a metabolic pathway to be established appeared feasible from all assessed carbon-sources. This means that the targeted non-natural bio-polyesters can theoretically be produced *de novo*, without the need for co-feeding of polymer precursors, given that (A) metabolic engineering efforts to produce the monomers are successful and (B) these are polymerizable, which will likely require further protein engineering of PHA synthases to expand the enzymes functionality.

Certain feedstocks appeared superior over others in terms of theoretical maximum yield: carbon-yields on formate were lowest, followed by acetate. Fructose and glycerol, as more reduced carbon-sources, could deliver higher yields, only surpassed by CO_2+H_2.[1] The near-100% carbon-efficiency on carboxy-hydrogen can be explained with the separation of carbon- and energy-source into two chemical species, allowing certain steady-state flux distributions where as much energy as needed was directed to recycling of CO_2, by means of the H_2 to CO_2 intake-ratio. This translates into an imperative for process control to optimize the gas-mix and/or implement effective recycling of unused substrate. The marginal yields on formate are owed to the low energy that is chemically bound by the combined carbon- and energy-carrier. Much of it is simply converted to carbon dioxide to obtain reducing equivalents to drive metabolism and little of it can be assimilated, which equals a scenario of carboxy-hydrogen feed with fixed ratio. Nevertheless, as formate can be produced electrochemically from carbon dioxide (35), recycling the inorganic carbon in a closed loop system could effectively create an analogous “open ratio” scenario where overall carbon-yields should approach those on carboxy-hydrogen (if a technical solution that is economical can be developed).

[1] When interpreting these results, it should be kept in mind that the model does not predict the phenotype that can be expected but is reflective of the leeway of the microbial system (i.e., cellular metabolism). In reality, many other factors can influence the actual idle state of the system, including kinetics (cf. rate-yield trade-off), which are not respected in this particular type of metabolic model.

Conclusion

We designed the first microbial cell factory capable of synthesizing a biological polymer with an aromatic ring in its backbone. In this comprehensive study, production of a wide range of non-natural polyhydroxyalkanoates from sustainable feedstocks was studied *in vivo* and *in silico*. It appeared that enzyme expression-level and polymer chain-length were inversely correlated, which has wide-ranging implications for strain engineering – in particular, balancing of the catalytic rates in respect to the PHA synthase is thought to be crucial to fine-tune polymer quality.

In feeding experiments with engineered *C. necator* various non-natural copolymers of 3-hydroxybutyrate with hydroxy carbonic acids (aliphatic and aromatic) were formed. Aromatic 2-hydroxy carbonates with a phenyl-group on a side chain of two, one and without residual carbons could be incorporated in the polymer. In addition, a co-polymer containing the phenyl-group in the backbone of the polymer was formed, which could be described as a polyhydroxyarylate. This novelty paves the way towards biological production of high-strength liquid-crystal polymers. All precursors are bio-available from waste carbon-sources (e.g., lignin in case of phloretic acid (36, 37)) and/or can be biosynthesized *de novo* from one-carbon sources such as carbon dioxide. Deploying a bio-electrochemical system for cultivation of the transgenic microbial cell factory, only providing CO_2 and electricity for growth, showed that aromatic polyester can also be formed under autotrophic conditions. This opens the opportunity for truly sustainable biological production of renewable plastics.

Using metabolic pathway modelling, the potential for production of a wide range of bio-polyesters was analyzed in models of *C. necator* and found to be feasible. This highlights the potential for bio-production of the non-natural polyesters formed in this study as well as others, outgoing from sustainable carbon-sources, paving the way for creation of bioplastics with a wide range of properties. Extensive metabolic engineering will be required to realize the full *de novo* production of these polymers, however, recent development in synthetic biology and genetic tools, in particular for engineering of *C. necator,* indicate that this CO_2 valorization strategy is feasible and within reach (4, 21). The ability of the PHA synthase to polymerize various aromatic hydroxy acids and importantly *para*-hydroxyphenyl-compounds is auspicious, however, much advancement is still needed to reach polymers with a significant content of aromatic in the backbone and high molecular weight.

Overall, the here demonstrated production of novel biologically accessible aromatic polyesters presents an important step in the efforts to leverage the power of biomanufacturing for the carbon-neutral (and potentially even carbon-negative) production of bio-replacement materials in order to create a sustainable chemical industry and thereby circular economy.

Materials and Methods

Strains and Media

Rich Broth (RB) was composed of Nutrient Broth (16 g/L), Yeast Extract (10 g/L) and ammonium sulfate (5 g/L). When applicable, kanamycin (kan, 300 mg/L for *C. necator* and 100 mg/L for *E. coli*) and/or diaminopimelate (DAP, 300 µM / 100 mg/L) were added.

Modified Mineral Salts Medium (MSM) was based on literature (38) and contained 6.4 g/L Na_2HPO_4, 4.8 g/L KH_2PO_4, 2 g/L NH_4Cl, $MgSO_4$ 0.36 g/L, $CaCl_2{\times}2H_2O$ 0.088 g/L, 20 g/L fructose and 1 mL/L of 1000× trace elements (0.2 g/L $CoCl_2{\times}6H_2O$, 0.01 g/L $CuSO_4{\times}5H_2O$, 0.15 g/L $FeSO_4{\times}7H2O$, 0.06 g/L NH4Fe(III) citrate, 0.3 g/L H_3BO_4, 0.035 g/L $MnCl_2{\times}4H_2O$, 0.035 g/L $(NH_4)6Mo_7O_{24}{\times}4H_2O$, 0.031 g/L $NiSO_4{\times}7H_2O$, 0.1 g/L $ZnSO_4{\times}7H_2O$). The medium was supplemented with kanamycin (300 mg/L) when applicable to ensure plasmid maintenance.

For (electro)autotrophic cultivations modified minimal medium that contained no chlorine salts to avoid electrocatalytic Cl_2 formation, was adapted from literature (39). Specifically, the electro-medium contained 4.52 g/L Na_2HPO_4, 5.17 g/L $NaH_2PO_4{\times}2H_2O$, 0.17 g/L K_2SO_4, 0.097 g/L $CaSO_4{\times}2H_2O$, 0.8 g/L $MgSO_4{\times}7H_2O$, 0.94 g/L $(NH_4)_2SO_4$ and 350 µL/L of 2857× of trace elements (10 g/L $FeSO_4{\times}7H_2O$, 2.4 g/L $MnSO_4{\times}H_2O$, 2.4 g/L $ZnSO_4{\times}7H_2O$, 0.48 g/L $CuSO_4{\times}5H_2O$, 1.8 g/L $Na_2MoO_4{\times}2H_2O$, 1.5 g/L $NiSO_4{\times}6H_2O$, 0.04 g/L $Co(NO_3)_2{\times}H_2O$ in 0.1 M HCl). The medium was supplemented with kanamycin (100 mg/L) to ensure plasmid maintenance. For production of PHA in the bio-electrochemical system (BES), the initial concentration of $(NH_4)_2SO_4$ was further reduced to 5 mM to achieve nitrogen-limiting conditions.

E. coli WM3064, a B2155 derivative, an auxotrophic RP4 mobilizing λ*pir* cell-line (thrB1004 pro thi rpsL hsdS lacZΔM15 RP4-1360 Δ(araBAD)567 ΔdapA1341::[erm pir]), was a gift from the Spormann Laboratory (Stanford University). WM3064 was routinely cultivated on LB (solid or liquid, at 30°C) supplemented with DAP (300 µM) and kanamycin (50 µg/mL) as applicable. *C. necator* H16 and *C. necator* H16 Δ*phaC1* were gifts from the Silver Laboratory (Harvard Medical School) (22) and routinely grown at 30°C on solid or liquid RB or MSM. A comprehensive list of the strains used and constructed in this study can be found in table 2.

Table 2: strains used in this study.

Strain	Genotype	Source
E. coli WM3064		(40)
E. coli WM3064 pCM66T_P_{BAD}-RFP		this study
E. coli WM3064 pCM66T_P_{BAD}-*pct540-phaC1437*		this study
E. coli WM3064 pCM66T_P_{BAD}-*hadA-phaC1437*		this study
C. necator H16		
C. necator H16 Δ*phaC1*	H16 Δ*phaC1*	(22)
C. necator H16 Δ*phaC1* pCM66T_P_{BAD}-RFP	H16 Δ*phaC1* RFP	this study
C. necator H16 Δ*phaC1* pCM66T_P_{BAD}-*pct540-phaC1437*	H16 Δ*phaC1 pct540 phaC1437*	this study
C. necator H16 Δ*phaC1* pCM66T_P_{BAD}-*hadA-phaC1437*	H16 Δ*phaC1 hadA phaC1437*	this study

Genetic Engineering

Vector Construction

The RK2/RP4 oriV (IncP) plasmid pCM66T was obtained from AddGene. pBBR1MCS_P_{BAD}-RFP, a derivate of pBBR1MCS with a red fluorescent protein (RFP) under control of the araBAD promoter, was a gift from the Silver Laboratory (Harvard Medical School). pCM66T_P_{BAD}-RFP was constructed by cloning the P_{BAD}-RFP cassette into pCM66T using NEBuilder, replacing the polylinker and its regulatory elements. The protein sequences of Q9L3F7_CLOPR (*pct*), Q188I3_PEPD6 (*hadA*) and B9W0T0_9PSED (*phaC*) were derived from UniProt, implementing the previously described mutations (V193A for *pct540* and E130D, S325T, S477G, Q481K for *phaC1437*) as applicable. The sequences were fused with a C-terminal tripleglycine-spacer and tetracysteine- (Lumio)-tag and codon-optimized for expression in *C. necator* with GeneArt® (Invitrogen). The genes were arranged in a single operon under control of the araBAD promoter in combination with the strong T7 ribosomal binding-site and a T7Te – rrnB T1 double-terminator. The plasmids pCM66T_P_{BAD}-*pct540-phaC1437* and pCM66T_P_{BAD}-*hadA-phaC1437* were constructed by GenScript, cloning the synthetic operons containing *pct540* & *phaC1437* and *hadA* & *phaC1437*, respectively, into pCM66T_P_{BAD}-RFP (cf. supplementary material 2).

Conjugation

Plasmid vectors were introduced into *C. necator* by conjugation, using the *E. coli* donor-strain WM3064, which had been transformed with the plasmid vectors pCM66T_P_{BAD}-*pct540-phaC1437* and pCM66T_P_{BAD}-*hadA-phaC1437* using the Mix & Go! *E. coli* Transformation Kit (Zymo).

Conjugation was performed as follows: The recipient strain (H16 Δ*phaC1*) was incubated at 30°C on RB plates for two days, simultaneously the donor strains carrying the plasmid vectors were incubate at 37°C on LB + Kan + DAP plates for one day. On the third day the donor strains were inoculate in liquid LB + Kan + DAP and incubated overnight with shaking at 37°C, the recipient strain was inoculated in RB and incubate overnight with shaking at 30°C. On the fourth day 3 mL of LB + DAP (but no antibiotics) were inoculated with 6 µL of each overnight donor-strain culture and incubated with shaking at 37°C. At the same time 20 µL of overnight *C. necator* culture was added in 10 mL RB and incubated at 30°C while shaking. After 4 h 3 mL of the *E. coli* and 10 mL of the *C. necator* culture were combined and spun down (4816 g for 10 min). The supernatant was discarded, and the cells were re-suspended in 200 µL RB + DAP. A "blob" of the cell mixture was pipetted on an RB + DAP plate and incubated at 30°C overnight (face of plate up). On day five all of the grown biomass was collected from the overnight plate with an inoculation loop and suspended into 500 µL of 25% glycerol and diluted 1:10 and 1:100. All three concentrations were plated on separate RB + kan plates. The plates were incubated at 30°C, colonies that appeared after 2-3 days were picked and isolated on separate RB + kan plates for screening.

Cultivation of Microbes

Cultivation of *C. necator* in Shake- and Serum-Flasks

Liquid cultures under heterotrophic conditions were conducted in 500 mL vented, baffled shake-flasks (WHEATON® Erlenmeyer Flasks with DuoCap®, DWK Life Sciences), incubated with shaking at 180 rpm on an innova 2300 platform shaker (New Brunswick Scientific) at 30°C. For feeding experiments, precultures of the engineered *C. necator* strains were inoculated in liquid RB + kan (50 mL) from solid RB + kan and grown over-night. In the morning the medium was exchanged for MSM + kan, diluting the culture 1:2 (in 100 mL). In the afternoon the seed-culture was washed with MSM and again diluted 1:2 (in 200 mL) with MSM + kan + polymer-precursor and induced with arabinose (1 g/L, unless indicated otherwise) in the evening. OD was monitored accompanied by collection of supernatant samples. The cultures were harvest after approx. 48 h or when no more increase in biomass was observed for 12 h.

Precultures for the bio-electrochemical system were done in two steps: 125 mL serum bottles (25 mL liquid medium, 100 mL gas headspace) were filled with 25 mL electro-medium and sealing with butyl rubber stopper and crimp-cap. Starting with fructose (1 g/L) as carbon-source, the medium was inoculated with *C. necator* H16 Δ*phaC1* pCM66T_P_{BAD}-*hadA*-*phaC1437* from solid RB + kan (heterotrophic growth) and incubated at 30°C with shaking at 200 rpm overnight. Subsequently, these cultures were transferred to autotrophic conditions on $H_2/CO_2/O_2$: the initial gas-phase was H_2/CO_2 (80%/20%) at 17 psi, which was further pressurized to 22 psi with O_2 (100%), resulting in a final gas composition of 64:16:20 ($H_2/CO_2/O_2$). After three days of incubation autotrophic growth was observed, reaching a maximum cell density of OD 3.8±0.15 within 48 h (data not shown). For transfer to the BES exponentially growing cultures were harvested at an OD of ≈ 0.7 (by centrifugation at 4000×g for 6 min) and re-suspended in 25 mL fresh medium.

Cultivation of *C. necator* in Bio-electrochemical System

The bio-electrochemical system was a custom (500 mL) glass vessel with rubber-stopper side ports (Adams & Chittenden Scientific). The reactor was operated membrane-less as three-electrode set up, magnetically stirred at 300 rpm. The cathode was a Nickel-Molybdenum alloy on graphite support (total surface area 50 cm^2), which has been characterized previously and found to evolve H_2 at 100% selectivity under biologically relevant conditions (41, 42). The anode was platinized titanium mesh (PLANODE1X4, TWL) and an Ag/AgCl reference electrode (NaCl saturated; RE-5B, BASi®), both of which were inserted via a rubber stopper side port. The electrochemical reactor was controlled by applying a constant current of 100 mA using a multichannel potentiostat (VMP3; BioLogic Science Instruments, EC-Lab 11.21). This way, a constant amount of electron flow and therefore constant flow of H_2 and O_2 was provided. In abiotic pre-tests (data not shown) the reactor headspace was analyzed (via GC) to confirm that H_2 and O_2 were the sole gaseous products. The reactor was filled with 300 mL medium, and CO_2 was supplied via a mass flow controller (EL-Flow F-100D, Bronkhorst®) at a constant flow rate of 1 mL/min. Before inoculation, the BES was operated for at least one hour under abiotic conditions to saturate the medium with the gases. The reactor was inoculated with 25 mL of concentrated cell-suspension from exponentially growing, autotrophic cultures, so that a starting OD between 0.5-0.6 (and final liquid volume of 325 mL) was

achieved. Preliminary tests showed that under autotrophic growth conditions accumulation of PHA required tight limitation of the nitrogen-source. Therefore, the initial concentration of ammonium salt in the BES was reduced to 5 mM and consumption was monitored ("EasyStrips" Ammonia Test Strips, Tetra® GmbH, sensitivity < 0.5 mg/L) throughout the experiment. Growth and pH were also measured by drawing samples manually. After 24 h the culture was induced with arabinose (0.1 g/L final conc.). 24 h after induction, the first dose of precursor was added (2.5 mM final conc.), and the second dose (additional 2.5 mM, i.e. 5 mM total) when the nitrogen-source was depleted. The experiment was terminated when the OD became stationery, cells were harvested via centrifugation followed by polymer extraction. Pictures of the set up can be found in supplementary material 1 (Figure S5).

Extraction of PHAs

Liquid culture of *C. necator* was harvested by centrifugation and the cell pellet was freeze dried. After determining the dry cell weight (CDW), PHAs were extracted by lysis of the cell pellet (wet or dry) with 10% sodium hypochlorite solution (Honeywell Fluka™) using approx. 0.2 L/g_{CDW}. The pellet was completely suspended and incubated at room-temperature for 20 min with intermittent mixing. The suspension was diluted with water 1:2 and centrifuged at 4816×g for 20 min. The remaining solids, containing the PHAs, were washed twice with water and once with methanol, repeating the centrifugation step. The dried PHA was weight to determine product yield, dissolved in chloroform, filtered with a 0.2 µm PTFE "Titan3™" (Thermo Scientific™) syringe filter and dried for analysis.

Protein Extraction and Detection

Culture derived from distinct time-points of a batch cultivation (exponential-phase / stationary-phase) was collected (sample volume [mL] ≈ 10 / OD_{600}) and cells were pellet by centrifugation (4816×g at 4°C for 10 min). The pellet was washed with purified water and stored as cell-paste at -20°C for later processing. For extraction of proteins, CelLytic™ B (Sigma) was used as per manufacturer's directions (approx. 1 mL per cells from 10 mL culture at an OD of 1), in combination with Protease Inhibitor Cocktail (Sigma-Aldrich). The mixture was vortexed for 2 min to lyse cells and extract the soluble protein. Centrifugation (4816×g for 10 min) pelleted the cell debris; the supernatant, which contained the soluble proteins, was separated. Total protein concentration was determined using the BCA Protein Assay Kit (Pierce™). Using the Lumio™ Green Detection Kit (ThermoFisher) as per manufacturer's directions 10 µg crude protein extract of each sample were prepared for gel electrophoresis. Size-separation was performed on a Bolt™ 4-12% Bis-Tris Plus Gel (ThermoFisher), run at 150 V for approx. 40 min with Bolt™ MES SDS Running Buffer (ThermoFisher). The marker was BenchMark™ Fluorescent Protein Standard (ThermoFisher). A Gel-Doc (BioRad) was used to visualize fluorescent-conjugated proteins. For visualization of all proteins, the gels were re-stained with One-Step Lumitein™ Protein Gel Stain (Biotium) as per manufacturer's directions and imaged again as before.

Analytics

Determination of OD and cell dry weight correlation

Microbial growth was characterized by measuring the optical density at 600 nm (OD_{600}) with a DR2800™ Portable Spectrophotometer (HACH) for shake-flask cultures and Ultrospec™ 2100 pro (Amersham BioSciences) in case of MES.

A correlation between OD_{600} and biomass (BM) concentration was determined gravimetrically (data not shown) from batch shake-flask cultivations with the wild-type (five samples) and engineered strains (five samples of the *pct540*-strain, 10 samples of the *hadA*-strain) of *C. necator*. Shake-flask cultures of 50 mL with different cell densities were harvested via centrifugation and vacuum dried. The average quotient of OD_{600}/BM (dry weight in mg) from the total of 20 samples was 0.3±0.04, such that the correlation is $OD_{600} \times 0.3$ = BM [g/L].

HPLC

Quantification of fructose in fermentation broth was based on a previously published HPLC-method for detection of organic acids (43). In short, the procedure was as follows: Samples (1 mL) were filtered (PVDF or PES syringe filters, 0.2 µm pore-size) and diluted 1:100 into HPLC sampling vials. Analysis of 50 µL sample-volume was performed on an 1260 Infinity HPLC system (Agilent), using an Aminex HPX87H column (BioRad) with 5 mM H_2SO_4 as the eluent, at a flow rate of 0.7 mL/min. Fructose was identified and quantified by comparison to standards (3 g/L, 1.5 g/L, 0.6 g/L, 0.3 g/L, 0.15 g/L, 0.03 g/L), according to retention time (8.8 min) using a refractive index detector (35°C).

Nuclear Magnetic Resonance (NMR) Spectroscopy

NMR samples were prepared as previously reported (44). In short, a few mg of polymer were dissolved in deuterated chloroform and ^{1}H-NMR as well as ^{13}C-NMR spectra were recorded at 25°C on a Unity INOVA™ 500 NMR Spectrometer (Varian Medical Systems) with chemical shifts referenced in ppm relative to tetramethylsilane.

Gas Chromatography–Mass Spectrometry (GC-MS)

GC-MS analysis was adopted from literature (22). Between 3-70 mg of extracted PHAs were transferred to crimped vials and 2 mL chloroform + 2 mL methanol with 15% HCl was added. The vials were closed and incubated for 1-2 h at 100°C. Vials were cooled on ice and content was combined with 4 mL H_2O in a screw cap glass vial. The mixture was vortexed and phases were separated by centrifugation at 3000 rpm for 10 min. The lower chloroform phase was transferred into a GC-MS vial for analysis. Samples were analyzed on a 7890 / 5975 inert XL GCMS (Agilent Technologies) with a J&W CP-TAP CB column CP7483 (Agilent Technologies). Analytes were heated on a gradient from 35-250°C at 2°C/min. Copolymers were detected with mass spectra of hydroxy acid methyl esters at m/z = 1-3 and NIST Mass Spectral Library.

Gel Permeation Chromatography (GPC)

Polystyrene calibrated (from M_p = 500-275,000 g/mol) molecular weights were determined using a GPCmax autosampler (Viscotek) with 300 mm × 7.7 mm GPC column (Waters™) in $CHCl_3$ at 25°C at a flow rate of 1 mL/min and S3580 refractive index detector (Viscotek).

Metabolic Modelling

Based on previously established metabolic networks of *C. necator* for elementary flux-mode analysis (45, 46), the present model was fundamentally re-constructed, refined and fully compartmentalized. Expansions were made to describe C1- and energy-metabolism more precisely (26, 47) and the model was amended with additional carbon assimilation and product formation pathways (cf. supplementary material 1, figure S5), deducted from metabolic databases such as KEGG (48, 49). Reaction thermodynamics of the heterologous pathways were verified with eQuilibrator (50).

Elementary flux modes were calculated in MATLAB® (MathWorks®), using 'FluxModeCalculator' (51), and evaluated as described previously (52). Balances were established around boundary reactions, allowing carbon-yields [C-mol/C-mol] for all products to be determined.

Supporting Information

- Appendix: Documentation containing growth-data and protein gels, NMR & GC-MS spectra and extended GPC data (supplementary material 1)

- Datasets: Annotated vector maps of genetic constructs (supplementary material 2) & spreadsheet containing metabolic models of *C. necator* (supplementary material 3)

Acknowledgements

This study was supported by a Stanford Natural Gas Initiative (NGI) program grant (SPO #139138), as well as NASA grant or cooperative agreement award number NNX17AJ31G. Any opinions, findings, and conclusions or recommendations expressed in this material are those of the author and do not necessarily reflect the views of the National Aeronautics and Space Administration (NASA).

Author Contributions

NJHA conceived the study, designed, and conducted the experiments and composed the manuscript. VEP, FK, MZ performed analytics (NMR & GPC, HPLC, GC-MS, respectively), SNN helped with strain construction. FK designed and conducted experiments in the bio-electrochemical system. RWW and CSC supported and advised the project. All authors have read and approved the final manuscript.

Competing Interests

The authors declare no competing interests.

References

1. J. Smith, S. Vignieri, A devil's bargain. *Science* **373**, 34-35 (2021).
2. S. R. Nicholson, N. A. Rorrer, A. C. Carpenter, G. T. Beckham, Manufacturing energy and greenhouse gas emissions associated with plastics consumption. *Joule* **5**, 673-686 (2021).
3. R. Geyer, J. R. Jambeck, K. L. Law, Production, use, and fate of all plastics ever made. *Science Advances* **3**, e1700782 (2017).
4. S. Y. Lee *et al.*, A comprehensive metabolic map for production of bio-based chemicals. *Natue Catalysis* **2**, 18-33 (2019).
5. X. Chen, N. Yan, A brief overview of renewable plastics. *Materials Today Sustainability* **7-8**, 100031 (2020).
6. L. D. Ellis *et al.*, Chemical and biological catalysis for plastics recycling and upcycling. *Nature Catalysis* **4**, 539-556 (2021).
7. G. Atiwesh, A. Mikhael, C. C. Parrish, J. Banoub, T.-A. T. Le, Environmental impact of bioplastic use: A review. *Heliyon* **7**, e07918 (2021).
8. J. M. Clomburg, A. M. Crumbley, R. Gonzalez, Industrial biomanufacturing: The future of chemical production. *Science* **355**, aag0804 (2017).
9. A. M. Brandon, C. S. Criddle, Can biotechnology turn the tide on plastics? *Curr Opin Biotech* **57**, 160-166 (2019).
10. P. J. Strong *et al.*, The Opportunity for High-Performance Biomaterials from Methane. *Microorganisms* **4**, 11 (2016).
11. Z. Li, J. Yang, X. J. Loh, Polyhydroxyalkanoates: opening doors for a sustainable future. *NPG Asia Materials* **8**, e265-e265 (2016).
12. B. Andreeßen, N. Taylor, A. Steinbüchel, V. Müller, Poly(3-Hydroxypropionate): a Promising Alternative to Fossil Fuel-Based Materials. *Applied and Environmental Microbiology* **80**, 6574-6582 (2014).
13. C. Utsunomia, Q. Ren, M. Zinn, Poly(4-Hydroxybutyrate): Current State and Perspectives. *Frontiers in Bioengineering and Biotechnology* **8** (2020).
14. A. G. Aduhene *et al.*, Poly(3-hydroxypropionate): Biosynthesis Pathways and Malonyl-CoA Biosensor Material Properties. *Frontiers in Bioengineering and Biotechnology* **9** (2021).
15. M. Ishii-Hyakutake, S. Mizuno, T. Tsuge, Biosynthesis and Characteristics of Aromatic Polyhydroxyalkanoates. *Polymers* **10**, 1267 (2018).
16. T. Liu *et al.*, Synthesis of Polymandelide: A Degradable Polylactide Derivative with Polystyrene-like Properties. *Macromolecules* **40**, 6040-6047 (2007).
17. T. L. Simmons, G. L. Baker, Poly(phenyllactide): Synthesis, Characterization, and Hydrolytic Degradation. *Biomacromolecules* **2**, 658-663 (2001).
18. J. E. Yang *et al.*, One-step fermentative production of aromatic polyesters from glucose by metabolically engineered Escherichia coli strains. *Nat Commun* **9**, 79 (2018).
19. X. Jin, C. Carfagna, L. Nicolais, R. Lanzetta, Synthesis and characterization of potentially biodegradable thermotropic polyesters based on *p*-hydroxybenzoic acid and glycolic acid. *Journal of Polymer Science Part A: Polymer Chemistry* **32**, 3115-3122 (1994).
20. A. Reina, A. Gerken, U. Zemann, H. R. Kricheldorf, New polymer syntheses, 101. Liquid-crystalline hyperbranched and potentially biodegradable polyesters based on phloretic acid and gallic acid. *Macromolecular Chemistry and Physics* **200**, 1784-1791 (1999).
21. J. Panich, B. Fong, S. W. Singer, Metabolic Engineering of *Cupriavidus necator* H16 for Sustainable Biofuels from CO2. *Trends in Biotechnology* **39**, 412-424 (2021).
22. S. N. Nangle *et al.*, Valorization of CO2 through lithoautotrophic production of sustainable chemicals in *Cupriavidus necator*. *Metabolic Engineering* **62**, 207-220 (2020).
23. S. J. Park *et al.*, Metabolic engineering of *Ralstonia eutropha* for the production of polyhydroxyalkanoates from sucrose. *Biotechnology and Bioengineering* **112**, 638-643 (2015).
24. S. Mizuno, A. Hiroe, T. Fukui, H. Abe, T. Tsuge, Fractionation and thermal characteristics of biosynthesized polyhydoxyalkanoates bearing aromatic groups as side chains. *Polymer Journal* **49**, 557-565 (2017).
25. T. H. Yang *et al.*, Biosynthesis of polylactic acid and its copolymers using evolved propionate CoA transferase and PHA synthase. *Biotechnology and Bioengineering* **105**, 150-160 (2010).
26. N. J. Claassens *et al.*, Phosphoglycolate salvage in a chemolithoautotroph using the Calvin cycle. *Proceedings of the National Academy of Sciences* **117**, 22452-22461 (2020).
27. T. Tsuge, K. Tanaka, M. Shimoda, A. Ishizaki, Optimization of l-lactic acid feeding for the production of poly-d-3-hydroxybutyric acid by *Alcaligenes eutrophus* in fed-batch culture. *Journal of Bioscience and Bioengineering* **88**, 404-409 (1999).
28. S. L. Riedel, J. Lu, U. Stahl, C. J. Brigham, Lipid and fatty acid metabolism in *Ralstonia eutropha*: relevance for the biotechnological production of value-added products. *Applied Microbiology and Biotechnology* **98**, 1469-1483 (2014).
29. T. Fukui, M. Suzuki, T. Tsuge, S. Nakamura, Microbial Synthesis of Poly((R)-3-hydroxybutyrate-co- 3-hydroxypropionate) from Unrelated Carbon Sources by Engineered *Cupriavidus necator*. *Biomacromolecules* **10**, 700-706 (2009).

30. N. Lindenkamp, M. Schürmann, A. Steinbüchel, A propionate CoA-transferase of *Ralstonia eutropha* H16 with broad substrate specificity catalyzing the CoA thioester formation of various carboxylic acids. *Applied Microbiology and Biotechnology* **97**, 7699-7709 (2013).
31. A. Hiroe, K. Tsuge, C. T. Nomura, M. Itaya, T. Tsuge, Rearrangement of gene order in the phaCAB operon leads to effective production of ultrahigh-molecular-weight poly[(R)-3-hydroxybutyrate] in genetically engineered *Escherichia coli*. *Appl Environ Microbiol* **78**, 3177-3184 (2012).
32. K. K. Sakimoto *et al.*, Physical Biology of the Materials–Microorganism Interface. *Journal of the American Chemical Society* **140**, 1978-1985 (2018).
33. T. Krieg, A. Sydow, S. Faust, I. Huth, D. Holtmann, CO2 to Terpenes: Autotrophic and Electroautotrophic α-Humulene Production with *Cupriavidus necator*. *Angewandte Chemie International Edition* **57**, 1879-1882 (2018).
34. C. Liu, B. C. Colón, M. Ziesack, P. A. Silver, D. G. Nocera, Water splitting–biosynthetic system with CO2 reduction efficiencies exceeding photosynthesis. *Science* **352**, 1210-1213 (2016).
35. M. F. Philips, G.-J. M. Gruter, M. T. M. Koper, K. J. P. Schouten, Optimizing the Electrochemical Reduction of CO2 to Formate: A State-of-the-Art Analysis. *ACS Sustainable Chemistry & Engineering* **8**, 15430-15444 (2020).
36. G. T. Beckham, C. W. Johnson, E. M. Karp, D. Salvachúa, D. R. Vardon, Opportunities and challenges in biological lignin valorization. *Current Opinion in Biotechnology* **42**, 40-53 (2016).
37. A. J. Ragauskas *et al.*, Lignin Valorization: Improving Lignin Processing in the Biorefinery. *Science* **344**, 1246843 (2014).
38. Y.-H. Yang *et al.*, Optimization of growth media components for polyhydroxyalkanoate (PHA) production from organic acids by *Ralstonia eutropha*. *Applied Microbiology and Biotechnology* **87**, 2037-2045 (2010).
39. A. Sydow, T. Krieg, R. Ulber, D. Holtmann, Growth medium and electrolyte-How to combine the different requirements on the reaction solution in bioelectrochemical systems using *Cupriavidus necator*. *Eng Life Sci* **17**, 781-791 (2017).
40. C. Dehio, M. Meyer, Maintenance of broad-host-range incompatibility group P and group Q plasmids and transposition of Tn5 in *Bartonella henselae* following conjugal plasmid transfer from *Escherichia coli*. *Journal of Bacteriology* **179**, 538-540 (1997).
41. F. Kracke *et al.*, Robust and biocompatible catalysts for efficient hydrogen-driven microbial electrosynthesis. *Communications Chemistry* **2**, 45 (2019).
42. F. Kracke, J. S. Deutzmann, W. Gu, A. M. Spormann, *In situ* electrochemical H2 production for efficient and stable power-to-gas electromethanogenesis. *Green Chemistry* **22**, 6194-6203 (2020).
43. S. T. Lohner, J. S. Deutzmann, B. E. Logan, J. Leigh, A. M. Spormann, Hydrogenase-independent uptake and metabolism of electrons by the archaeon *Methanococcus maripaludis*. *The ISME Journal* **8**, 1673-1681 (2014).
44. J. Myung *et al.*, Long-term cultivation of a stable *Methylocystis*-dominated methanotrophic enrichment enabling tailored production of poly(3-hydroxybutyrate-co-3-hydroxyvalerate). *Bioresource Technology* **198**, 811-818 (2015).
45. N. J. H. Averesch, F. Kracke, Metabolic Network Analysis of Microbial Methane Utilization for Biomass Formation and Upgrading to Bio-Fuels. *Frontiers in Energy Research* **6** (2018).
46. P. Unrean, K. L. Tee, T. S. Wong, Metabolic pathway analysis for *in silico* design of efficient autotrophic production of advanced biofuels. *Bioresources and Bioprocessing* **6**, 49 (2019).
47. R. Cramm, Genomic View of Energy Metabolism in *Ralstonia eutropha* H16. *Microbial Physiology* **16**, 38-52 (2009).
48. M. Kanehisa, S. Goto, KEGG: Kyoto Encyclopedia of Genes and Genomes. *Nucleic Acids Res* **28**, 27-30 (2000).
49. H. Ogata *et al.*, KEGG: Kyoto Encyclopedia of Genes and Genomes. *Nucleic Acids Res* **27**, 29-34 (1999).
50. A. Flamholz, E. Noor, A. Bar-Even, R. Milo, eQuilibrator—the biochemical thermodynamics calculator. *Nucleic Acids Res* **40**, D770-D775 (2011).
51. J. B. van Klinken, K. Willems van Dijk, FluxModeCalculator: an efficient tool for large-scale flux mode computation. *Bioinformatics* **32**, 1265-1266 (2015).
52. I. Vassilev, N. J. H. Averesch, P. Ledezma, M. Kokko, Anodic electro-fermentation: Empowering anaerobic production processes via anodic respiration. *Biotechnology Advances* **48**, 107728 (2021).